

1                   **Tunable Acoustic Properties in Reconfigurable Kerf Structures**

2  
3                   Di Liu<sup>1</sup>, Zaryab Shahid<sup>2</sup>, Yung-Hsin Tung<sup>3</sup>, Anastasia Muliana<sup>4</sup>, Youngjib Ham<sup>5</sup>, Negar  
4                   Kalantar<sup>6</sup>, Theodora Chaspari<sup>7</sup>, Ed Green<sup>8</sup>, James E. Hubbard<sup>9</sup>

5  
6                   **Abstract**

7                   Freeform structures are appealing in architecture owing to their ability to combine pleasing  
8                   aesthetics and functionality. Regarding architectural functionality, freeform structures have the  
9                   potential to meet desired acoustic requirements in indoor architecture through the proper design of  
10                  materials and geometries. Kerfing is one of the practical methods to generate reconfigurable  
11                  freeform structures from rigid planar construction materials. This study aims to explore tunable  
12                  room acoustic characteristics through the use of kerf structures. In this study, we investigate  
13                  acoustic responses of kerf structures out of a medium density fiber (MDF) board having a hexagon  
14                  spiral kerf pattern with varying cut densities. Experiments are conducted to measure the acoustic  
15                  properties (e.g., absorption coefficient) of the kerf unit cells with different cut densities. We then

---

<sup>1</sup>Ph.D. Student, Department of Construction Science, Texas A&M University, 3137 TAMU, College Station, TX 77843; E-mail: [catsquito@tamu.edu](mailto:catsquito@tamu.edu)

<sup>2</sup>Ph.D. Student, J. Mike Walker '66 Dept. of Mechanical Engineering, Texas A&M University, College Station, TX, 77843, U.S.A., email: [zaryab94@tamu.edu](mailto:zaryab94@tamu.edu)

<sup>3</sup>Former Bachelor Student, Department of Multidisciplinary Engineering, Texas A&M University, College Station, TX, 77843, U.S.A., email: [yhc.tung@tamu.edu](mailto:yhc.tung@tamu.edu)

<sup>4</sup>Linda & Ralph Schmidt '68 Professor, J. Mike Walker '66 Dept. of Mechanical Engineering, Texas A&M University, College Station, TX, 77843, U.S.A., email: [amuliana@tamu.edu](mailto:amuliana@tamu.edu)

<sup>5</sup>History Maker Homes Endowed Associate Professor, Department of Construction Science, Texas A&M University, 3137 TAMU, College Station, TX 77843; E-mail: [yham@tamu.edu](mailto:yham@tamu.edu) (Corresponding Author)

<sup>6</sup>Associate Professor, Architecture Division, California College of the Arts, San Francisco, CA 94107, U.S.A., email: [kalantar@cca.edu](mailto:kalantar@cca.edu)

<sup>7</sup>Assistant Professor, Department of Computer Science and Engineering, Department of Computer Science and Engineering, Texas A&M University, College Station, TX, 77843, U.S.A., email: [chaspari@tamu.edu](mailto:chaspari@tamu.edu)

<sup>8</sup>Principal Consultant, Hottinger Brüel & Kjaer Inc, Canton, MI, 48187, U.S.A., email: [ed.green@hbkworld.com](mailto:ed.green@hbkworld.com)

<sup>9</sup>Professor, J. Mike Walker '66 Dept. of Mechanical Engineering, Texas A&M University, College Station, TX, 77843, U.S.A., email: [jhubbard@tamu.edu](mailto:jhubbard@tamu.edu)

16 design kerf patterns using the parametric design method and explore the flexibility of kerf  
17 structures with different kerf cut densities. We model the kerf structures of varying kerf cut density  
18 and shape reconfiguration and use a ray-tracing simulation to study their impacts on the acoustic  
19 performance i.e., reverberation times (RT) of a small office space. Overall, this study leverages  
20 the unique attributes of kerf structures such as different cut densities and shape reconfigurations  
21 to tune the room acoustics in addition to their usage in indoor architectures due to their pleasing  
22 aesthetics.

23

## 24 **1. Introduction and Background**

25 The acoustic performance is a major component of the architectural design that should consider  
26 occupant's comforts and needs (Varjo et al. 2015). For example, noise pollution in space is  
27 detrimental to the occupants' performance, health, and well-being. Moreover, a study has shown  
28 that increasing human performance in an office environment can boost the U.S. economy by \$450  
29 to \$550 billion annually (Hung 2017). Architects and acousticians have developed various types  
30 of materials and structural configurations to meet the acoustic requirements of indoor spaces.  
31 Recently, freeform structures which are known for their aesthetic appeal are primarily being used  
32 in indoor architectures to control acoustic performance. For example, Vercammen used concave  
33 and convex surfaces which can focus and diffuse the sound waves, thus, amplifying and reducing  
34 the sound effects as desired (Vercammen 2013). Similarly, Peters et al. designed, fabricated, and  
35 tested responsive acoustic surfaces which is a system of trihedral folded plates that have hard  
36 reflective Dibond and sound absorbent surfaces to create sound-amplified and sound-dampened  
37 zones respectively (Peters 2011). Belanger et al. studied the effect of curvature on the acoustic  
38 properties of glass panes formed by the combination of parametrically driven auxetic pattern

39 generation (Belanger 2018). They concluded that the curved panes could influence the room  
40 acoustics, as well as control the distribution of acoustic energy.

41 The kerfing technique, also known as relief cutting, is used to create flexible freeform  
42 structures from stiff planar materials such as metal and processed woods (Medium Density  
43 Fiberboard (MDF), plywood) (Zarrinmehr et al. 2017a; b; c). The kerf structures are commonly  
44 used in both indoor and outdoor architectural design due to their pleasing aesthetics and their  
45 ability to be reconfigured in any complex nonplanar shape (**Fig. 1.**). There are a variety of complex  
46 kerf patterns such as spiral, Archimedean squares, and hexagon patterns (Capone and Lanzara  
47 2018; Kalantar and Borhani 2018). The interplay between kerf patterns and cut densities is used  
48 to vary the stiffness of the kerf structures (Chen et al. 2020). As the kerf structures can be easily  
49 reconfigured into any non-planar shape, they have the potential to vary the acoustic environment  
50 of the space on demand. Recently, Holterman experimentally studied sound absorption coefficients  
51 and reverberation times of kerf cells and beams with different cut gaps and bending curvatures at  
52 frequencies 125-4000 Hz. Varying cut gaps and bending curvatures altered the reverberation time  
53 and absorption coefficients, and the amount of changes was frequency-dependent (Holterman  
54 2018). Overall, Holterman's study showed the potential of kerf structures in manipulating room  
55 acoustic characteristics. Future study needs to investigate the influence of multiple kerfing  
56 parameters such as the kerf density, kerf pattern, and shape reconfiguration on altering the acoustic  
57 properties of the kerf structures and their impact on room acoustic characteristics. Recent studies  
58 have shown that kerf-cut densities and materials influence the modal frequencies and shapes of the  
59 kerf cells and panels, and reconfiguring the cells and panel shapes altered the modal frequencies  
60 and shapes (Shahid et al. 2021, 2022b; a). These findings showed the potential of reconfiguring  
61 kerf cells and panels for tuning acoustic properties. Further investigation of these kerf parameters

62 is necessary as it not only allows the design researchers to clearly understand the dynamic relation  
63 between kerf structures and their acoustic responses but also enhances the adaptivity and  
64 responsivity of indoor acoustic design in practice. With an understanding of the overall effect of  
65 kerf structures on the indoor acoustic environment, architects and acousticians can deploy  
66 reconfigurable kerf structures according to the acoustic requirement of the indoor space.

67

## 68 **2. Kerf Structure**

69 Zarrinmehr et al. proposed an algorithm for remeshing 2D meander patterns to achieve local  
70 flexibility (Zarrinmehr et al. 2017b; c). Kerf patterns can be obtained from polygons such as  
71 Voronoi and hexagons. Kalantar et al. showed that facilitated with parametric adjustment, kerf  
72 panels can be utilized to create various types of formworks in architecture design to control the  
73 reconfigurability as desired (Kalantar and Borhani 2018). In this study, the hexagon spiral pattern  
74 is studied as shown in **Fig. 2**. The hexagon unit cell has a symmetric structure which makes it  
75 easier to layout and generates flexible kerf structures used in freeform architecture. The hexagon  
76 spiral pattern is laser cut on a stiff 3.175 mm thick MDF panel. The MDF is a composite material  
77 formed from chopped wood fibers pressed together and bonded with epoxy. MDF is a common  
78 material used in indoor architectures (Ivanovic-Sekularac et al. 2012; Jakimovska Popovska et al.  
79 2016). The basic mechanical properties of the MDF panel are that the elastic modulus is 4 GPa,  
80 Poisson's ratio is 0.25, the tensile strength is 18 MPa, and the ultimate tensile strain is 0.5%.

81 The large kerf structures studied in this paper are made up of a hexagonal domain with  
82 triangular unit cells which have a side length of 25.4 mm and thickness of 3.175 mm as shown in  
83 **Fig. 2**. The hexagonal domain with triangular unit cells can be cut with different kerf densities  
84 depending on the desired flexibility and load-bearing capability (Chen et al. 2020). In this study,

85 high density (HD), medium density (MD), and low density (LD) kerf densities are studied.  
86 Detailed information about the geometrical parameters of these kerf unit cells is shown in **Table**  
87 1. The HD cut unit cell has a higher number of cutlines per unit cell compared to an MD and LD  
88 unit cell which leads to its higher air gap area. The HD unit cell will be more flexible which  
89 increases its reconfigurability but decreases load-bearing capacity (**Fig. 2.**). Additionally, the ratio  
90 of the air gap to total surface area is highest for the HD unit cell which leads to higher absorption  
91 compared to other unit cells considered in this study.

92

### 93 **3. Methodology**

94 In this paper, we study the attributes of kerf structures such as kerf cut density and shape  
95 reconfiguration which can be used to tune the acoustics of an indoor space. The kerfing technique  
96 is used to develop flexible freeform structures with different kerf cut densities. In this study, the  
97 flexible form of the kerf structure is designed building on the algorithm developed in  
98 Grasshopper3D named Relief Cut (Kalantar and Borhani 2018; Zarrinmehr et al. 2017a; b; c).  
99 Subsequently, acoustic properties of kerf structures (e.g., absorption coefficient) are  
100 experimentally determined using a custom-built impedance tube. The experimentally determined  
101 absorption coefficients are used in the ray-tracing simulations to study the effects of cut density  
102 and shape reconfiguration of kerf structures on the indoor acoustic environment, i.e., office space.  
103 From the ray-tracing simulations, acoustic properties used for indoor spaces such as Reverberation  
104 Time (RT) are determined to understand the effect of both kerf densities and shape  
105 reconfigurations of kerf panels on the overall room acoustic characteristics. Among various types  
106 of acoustic measurements, it is well-accepted that reverberation time (RT) is one of the most used

107 metrics to reflect the room's acoustic performance in design. RT is quantified by material types  
108 and room geometries, and the range of RT is implemented depending on the room size and function.

109 The experimental tests for the absorption measurement of the kerf unit cells were  
110 performed at Brüel and Kjaer (B&K), Detroit, MI. A custom-built 3-D printed tube is used to test  
111 the specimens. The tube is connected with a 100 mm diameter B&K 4206T Impedance Tube using  
112 a reducer as shown in **Fig. 3**. The loudspeaker is placed at the bottom end of the setup and the kerf  
113 specimen is clamped in between the orange and black tube. The microphones are inserted at four  
114 different locations on the 3-D printed tube to measure the standing wave sound field and determine  
115 the absorption of the specimen. The 3200 Hz bandwidth is chosen for all the measurements and a  
116 similar procedure is repeated for different density kerf unit cells. Detailed discussion on the  
117 experimental test and characterization of the absorption coefficient is given in Olivieri et al. 2006.

118 The absorption coefficients for HD, MD, and LD MDF specimens are shown in **Table 2**.  
119 It can be noticed from the results that the LD unit cell has the highest absorption coefficient across  
120 the frequency range compared to HD and MD unit cells, although for frequencies 125 and 250 Hz,  
121 the difference in the absorption coefficients for HD, MD, and LD is not significant (less than 10%  
122 variation). As the LD unit cell has a more solid area (fewer cut lines) which leads to higher energy  
123 being absorbed and less sound energy being transmitted relatively, thus increasing the absorption  
124 coefficient. At the frequencies 500 and 1000 Hz, the absorption coefficients are relatively low (less  
125 than 0.5), which can result in more sound reflection compared to other frequencies, as will be  
126 shown later. We will explore whether kerf panels can be used to manipulate room acoustic  
127 properties at these frequencies. Additionally, the Noise Reduction Coefficient (NRC) is also  
128 calculated to compare the average absorption of kerf panels with different cut densities (**Table 2**).  
129 NRC is the average absorption coefficient from all frequencies.

130 **4. Investigating Reconfigurable Kerf Structures for Small Office Acoustic**

131 Small-sized office spaces, which are often found in renovated buildings, are commonly  
132 used for group study rooms or offices that can accommodate 2-4 occupants. Repurposing the  
133 spaces in renovated buildings can result in poor acoustic quality. Acoustic design for small office  
134 spaces preliminary focused on preventing undesired interior noise, ensuring speech intelligibility,  
135 and maintaining auditory comfort (Jaramillo and Steel 2015). The hearing frequency range is  
136 usually from 300 Hz to 3000 Hz (SEA n.d.) and the conversational speech frequencies are ranged  
137 from 250 Hz to 4000 Hz (Quam et al. 2012). It is well-accepted to use the reverberation time  
138 (RT60) which is the time required for sound in space to decay by 60 decibels (dB) to measure the  
139 room's acoustic performance. It has been recommended that the RT60 of indoor spaces should be  
140 less than 1 second (Jaramillo and Steel 2015). The space which has RT higher than 2 seconds is  
141 echoic, while lower than 0.3 seconds is acoustically dead. Some design guideline recommends the  
142 appropriate range of reverberation time for an office space is between 0.7s to 0.4s (Anna n.d.).  
143 According to WELL standard, indoor acoustic performance is specified by the optimal  
144 reverberation time to control the ambient noise and ensure the auditory comfort (“Reverberation  
145 time | WELL Standard” n.d.). The optimal reverberation time is associated with the room volume  
146 and function. For office and learning spaces no more than 260 m<sup>3</sup>, the optimal RT60 should be no  
147 more than 0.6s (“Reverberation time | WELL Standard” n.d.).

148 The kerf structures can be reconfigured into various shapes due to their flexible nature to  
149 potentially control the room acoustic. In this regard, we examine how this unique attribute of kerf  
150 structures affects the acoustic response of a small office space. Among different shapes, curved  
151 surfaces have a great influence on the room's acoustics. Convex and concave shapes can render  
152 acoustic performance to be absorptive and reflective, as well as create various aesthetic features

153 (Vercammen 2013; Wulfrank et al. 2014). Concave shapes can cause sound amplification on the  
154 focusing point; while convex shapes can diffuse the reflected sound in different directions and  
155 balance the uneven sound distribution (Wulfrank et al. 2014). The implementation of curved  
156 shapes is often limited by material reconfigurability. Rigid materials often require extra frame  
157 structures and fabrication techniques to build into a curved shape. Kerf structures can address the  
158 challenges in fabricating curved surfaces out of rigid panels as they can be designed with controlled  
159 flexibility by changing kerf cut densities to enable for forming desired curved shapes. The flexible  
160 kerf structures can be easily reconfigured to potentially tune room acoustic characteristics. Limited  
161 efforts have been made to investigate how the curved kerf structure affects the room's acoustic  
162 characteristics.

163 We implemented the reconfigurable kerf structure for small office space (3m x 3m x 3m)  
164 and assessed how the designed parameters, such as kerf-cut densities and shapes of  
165 reconfigurations (i.e., flat, convex, concave, and a combination of convex and concave), affected  
166 the RT60 by using raytracing method. Further, we evaluated if occupants could be affected  
167 differently when their spatial positions were changed in the same office space.

168

#### 169 **4.1. Ray-tracing method validation**

170 The acoustic evaluation of the kerf panels is performed using the ray-tracing method. The  
171 simulation is set up in Rhino3D for a small office with a size of 3m x 3m x 3m, which is commonly  
172 found in renovated buildings (Fig. 4.). Gypsum is selected as floor and wall materials. We first  
173 access if the different air gaps of kerf structures affect the acoustic results as well as the validation  
174 of the ray-tracing method. The air gap is measured by the distance between the ceiling and the  
175 suspended kerf structure. In the demonstration, the kerf panels suspended from the ceiling at 24,

176 12, and 6 mm are examined respectively. The measured absorption coefficients from the  
177 experimental tests are input into the model for the respective kerf density (**Table 2**). A point source  
178 of sound is located 0.5 m from the wall, and the receiver is at the center of the room as shown in  
179 **Fig. 4**. The positions of the sound source of the receiver mimic a simplified daily scenario with  
180 two people speaking in conversation, where the speaker is standing close to the wall and the  
181 listener is sitting in the center of the room. An acoustic simulation engine, the Pachyderm plugin  
182 in Rhino3D is used to conduct the ray-tracing simulations (Harten 2013). Convergence studies  
183 were conducted to empirically determine the sufficient numbers of rays and cut-off time, and in  
184 this study, 30,000 rays and a cut-off time of 10,000 ms were used for the ray-tracing simulations.

185 To validate the ray-tracing simulations, a theoretical model of the Eyring equation  
186 (Beranek 2006) is used to determine the reverberation time of a space having a solid MDF panel  
187 suspended at a 24 mm distance from the ceiling (Beranek 2006). The reverberation time from the  
188 ray-tracing simulation was compared to the one determined by the Eyring model. The Eyring  
189 equation uses absorption coefficients of the materials on the walls and ceiling materials to output  
190 the Reverberation Time. It is a common method used by acousticians to determine the  
191 reverberation time before using computer-aided simulation methods to understand the acoustic  
192 behavior of indoor space. It is evident from **Fig. 5**. that the ray-tracing simulations can capture the  
193 results from the Eyring equation at all frequencies. The percentage error of results between ray-  
194 tracing simulations and the Eyring equation at 125Hz, 500Hz, 1000Hz, and 2000Hz are less than  
195 5%. The reverberation time increases up to a maximum value at the 1000 Hz frequency band and  
196 it starts decreasing at higher frequency bands (>1000 Hz). The validation analysis also helped us  
197 decide on simulation parameters such as rays, and the cut-off time for ray-tracing simulations,  
198 which are mentioned earlier.

199

200 **4.2. Acoustic Performance for Different Air Gaps of Planar Kerf Panels**

201 The acoustic performance of different densities (HD, MD, LD) of planar kerf panels is  
202 evaluated through ray-tracing simulations. RT60 caused by different densities of kerf panels and  
203 positions of kerf panels is measured. The results are compared to the responses of the solid panel,  
204 as shown in **Fig. 6**. By leveraging the kerf process, lower reverberation times (under 1 second) are  
205 achieved compared to solid MDF panels suspended from the ceiling. Also noted that at frequencies  
206 lower than 500 Hz and 2000 Hz, the RT60 of this studied room is low (around or less than 0.3) for  
207 all kerf panels, which is attributed to the high absorption coefficient (**Table 2**), and thus no further  
208 intervention is needed to tune room acoustic at these frequencies.

209 We can also observe that the desired RT60 can be achieved by having different positions  
210 and cut densities of kerf panels. For example, the LD kerf panel position at 24 mm from the ceiling  
211 achieved the recommended reverberation time for the office (<0.7s). Therefore, based on RT60  
212 results in this analysis, the kerf panels suspended 24 mm will be a suitable option in indoor spaces  
213 where less echo and higher speech intelligibility is preferred. This analysis shows that varying the  
214 kerf cut density of the kerf panels has a marginal effect on RT60.

215

216 **4.3. Acoustic Performance for LD and HD Reconfigurable Non-planar Kerf Structures**

217 The reconfigurability of the kerf structure depends on the kerf-cut densities, higher cut  
218 density results in a more flexible panel, hence easier for shape reconfiguration into non-planar  
219 shapes. We used raytracing simulation to examine the influence of reconfiguring kerf panels on  
220 RT60 for a small-sized office. Specifically, we considered HD panels with the highest  
221 reconfigurability and LD panels with the lowest reconfigurability. Kerf panels suspended 24mm

222 from the ceiling are selected for the simulation. We compared the acoustic performance of the HD  
223 and LD kerf structures, with flat and non-planar reconfigurations. The kerf structures were  
224 generated in Grasshopper3d. Specifically, the non-planar reconfiguration is modeled with four  
225 convex and concave kerf structure units to achieve a balanced sound distribution (**Fig.7a.**). A point  
226 source of sound is located 0.5 m from the wall with a height of 1.67m to mimic a standing speaker,  
227 and the receiver is in the center of the room with a height of 1m to mimic a sitting listener. The  
228 reverberation time of these reconfigurations is simulated. Results are discussed in **Section 5**.

229

230 **4.4. Acoustic Performance for Reconfigurable Kerf Structures by Varying Occupant  
231 Positions**

232 As it is common for a small office space to have multiple occupants or room layouts, it is  
233 important to understand if the office acoustic is consistent or adaptive by changing listener  
234 positions. We examined if RT60 of different non-planar reconfigurations would be varied along  
235 with changing the position of occupants. Here the HD kerf structure with 24mm suspended from  
236 the ceiling is chosen due to the highest reconfigurability among all three densities (**Fig.2**). Three  
237 types of non-planar reconfigurations are modeled and assessed: (1) multi-uniform convex  
238 reconfiguration, (2) multi-uniform concave reconfiguration, and (3) multi-mixed reconfiguration.  
239 For each type, multiple convex and/or concave units were included as shown in **Fig.8**. The 3D  
240 shapes of these non-planar reconfigurations can be referred to in **Fig.7a**. An omnidirectional sound  
241 source is placed 1.67m high from the floor, 0.5 m from the front wall, and 1.5 m to both sidewalls  
242 (**Fig. 9**). The position of the sound source was decided to be close to the wall aiming to mimic the  
243 speech voice standing next to one side of the room. Two parameters are taken into consideration  
244 to position receivers, namely, receiver height ( $H_R$ ) and distance from a sound source to each

245 receiver ( $D_{SR}$ ). A total of four receivers at two heights (1m and 1.75m) are placed at 1m and 2m  
246 from the sound source, respectively (**Fig. 9, Table 3**). The first set of receivers, A ( $H_{R\_A} = 1.75m$ )  
247 and B ( $H_{R\_B} = 1$ ) are placed at 1 m from the sound source ( $D_{SR\_AB} = 1$ ). The second set of receivers,  
248 C ( $H_{R\_C} = 1.75m$ ) and D ( $H_{R\_D} = 1m$ ) are placed at 2m from the sound source ( $D_{SR\_CD} = 2$ ). We  
249 examined several multi-uniform and multi-mixed configuration cases combining multiple convex  
250 and concave reconfigurations to achieve balanced acoustic results for each receiver. To do so, the  
251 ceiling area is evenly divided into sub-regions along the u direction and v direction, in which both  
252  $u, v = 2, 3, 4, 5$  (**Fig.8**). For example, when  $u, v = 2$ , the ceiling is evenly divided into four sub-  
253 regions. Convex or concave units are placed at each sub-region. Ray-tracing simulations are  
254 performed in Pachyderm for all shape reconfigurations at all four positions and reverberation time  
255 is determined. Results are discussed in Section 5.

256

## 257 **5. Results and Discussion**

### 258 **5.1. Results of LD and HD Reconfigurable Non-planar Kerf Structures**

259 **Fig.7b.** shows the office acoustic performance with varying configurations of kerf structure  
260 among the different kerf-cut densities. Significant differences in RT can be found between the flat  
261 surface and non-planar reconfigurations at 500Hz and 1000Hz, and non-planar reconfiguration  
262 yields much lower RT values than the flat surface for both HD and LD kerf structures. For both  
263 non-planar reconfigurations, RT values at 500 Hz and 1000 Hz range from 0.49s to 0.65s,  
264 satisfying the office acoustic design requirement that the reverberation time is between 0.7s to 0.4s.  
265 Additionally, for LD and HD non-planar reconfigurations, the significant difference in RT60  
266 ( $>10\%$ ) can be found at 1000 Hz, and a marginalized difference (2% - 10%) can be found at 500  
267 Hz. However, in both LD and HD non-planar reconfigurations insignificant changes in RT60 are

268 seen at frequencies 125, 250, and 2000 Hz due to the high absorption coefficient (>0.5) at these  
269 frequencies. We conclude that for non-planar reconfigurations with four convex and concave units,  
270 kerf structures with different kerf-cut densities (HD and LD) can be used to tune RT60 to meet the  
271 office acoustic design requirement (0.7s to 0.4s) at 500Hz and 1000Hz which fall into the human  
272 hearing frequency range. Considering the HD kerf structure also has higher reconfigurability than  
273 the LD kerf structure, the HD structure is selected for the future reconfiguration test. This study  
274 also shows the potential of reconfiguring kerf panels to improve the room's acoustic condition at  
275 specific frequencies where an intervention is needed.

276

## 277 **5.2. Results of Reconfigurable Kerf Structures by varying Occupant positions**

278 It is evident from the results in **Fig. 10a** that reconfiguring kerf structures affects  
279 reverberation time. Although with reconfiguring the kerf ceiling, the trend of the reverberation  
280 time remained the same across the frequency range, the reverberation time varies for different  
281 shape configurations. Especially, for all twelve non-planar reconfigurations, the reverberation time  
282 shows a significant variation between different ceiling configurations at 500 Hz and 1000 Hz  
283 frequency bands among all four receiver positions. Due to the increase in overall surface area of  
284 3x3 concave and convex reconfigurations compared to 2x2 convex and concave configurations,  
285 the total absorption of the indoor space increases ( $A = S_n \alpha_n$ ). This leads to lower reverberation  
286 times for 3x3 concave and convex reconfigurations (0.51s at 500Hz, 0.6s at 1000Hz) compared to  
287 2x2 configuration (0.56s at 500Hz, 0.65s at 1000Hz), especially at 500Hz and 1000Hz. Similarly,  
288 the reverberation time declines from 3x3 mixed shape to 4x4 mixed shape and 5x5 mixed shape  
289 ceiling. The 5x5 mixed-shape ceiling results in the highest surface area which increases the total  
290 absorption and thus leads to the lowest reverberation time compared to all ceiling shape

291 reconfigurations investigated in this study. However, there is a marginal difference in  
292 reverberation times of 2x2 multi-uniform (convex, concave) and 2x2 multi-mixed configurations.  
293 Similarly, there is an insignificant difference between 3x3 multi-uniform (convex, concave) and  
294 3x3 multi-mixed configurations. This is because with the same number of sub-divisions, the total  
295 volume and surface areas of indoor space ( $A = S_n \alpha_n$ ) remain the same. Additionally, for all twelve  
296 non-planar reconfigurations, reverberation time remains similar at 125 Hz, 250 Hz, and 2000 Hz,  
297 which is attributed to the relatively high absorption coefficient of kerf panels at these frequencies  
298 as discussed above.

299 **Fig. 10b.** shows that RT60 is similar between different receiver positions. As the receiver  
300 heights or the distance between the receiver and sound sources are changed, the RT60 remains  
301 consistent. Thus, regardless of the receiver's spatial locations, the reverberation time declined as  
302 the ceiling area has increasingly reconfigured sub-divisions, and this is likely because of the small  
303 size of the room.

304 Overall, these results demonstrate that by reconfiguring the kerf structures into different  
305 geometrical shapes, the acoustic response of the indoor space can be altered depending on  
306 reconfigured space geometries and serve the specific purpose of the space. Considering the human  
307 hearing frequency range is usually from 300 Hz to 3000 Hz, the reconfigurability of kerf structures  
308 has the potential to actively adjust room acoustic characteristics to enhance the sound quality such  
309 as the RT60 at the frequency of 500Hz and 1000Hz to fulfill the hearing demand. Specifically, as  
310 the total area of the subdivided reconfigurable surface increases, the RT60 is lowered to optimize  
311 the acoustic performance. We can conclude that, for small office spaces, the reverberation time is  
312 dependent on the overall number of reconfigurable kerf units and independent of the occupant  
313 positions. Moreover, although a previous study shows that changes in reverberation time are

314 frequency-dependent (Holterman 2018), it is more likely to occur only at certain frequencies (i.e.,  
315 500Hz, 1000Hz in this case study). Since the reconfigurable kerf structure is composed of various  
316 numbers of kerf units ( $n \times n$ ), it has the potential to be rapidly assembled and deployed based on  
317 different morphological and acoustic considerations and can be implemented as temporary  
318 structures to adapt to rich spatial functions and aesthetic requirements in buildings.

319

## 320 **6. Conclusion**

321 In this study, we explored the ability of kerf structures to tune the room acoustics in addition to  
322 their usage in small office spaces due to their pleasing aesthetics. We designed kerf structures  
323 made up of MDF with several cut densities (HD, MD, LD). To measure the absorption of MDF  
324 kerf structures, we conducted experiments on kerf unit cells in a custom-built impedance tube. To  
325 investigate how the kerf structure can improve the indoor acoustic for a small office, we modeled  
326 a small office space with kerf structures suspended from the ceiling with different kerf cut densities.  
327 The ray-tracing simulations are performed to determine reverberation time in the space having kerf  
328 panels installed on the ceiling. The measured absorption coefficients were used as input material  
329 parameters in the simulations. The results from these simulations demonstrate that the kerf cut  
330 densities affect the room's acoustic characteristics. As kerf structures are flexible and can be  
331 reconfigured to arbitrary freeform shapes, we investigated this attribute of kerf structures in  
332 altering the room's acoustic characteristics. We first investigated the compensated acoustic  
333 response caused by reconfigurability and kerf-cut densities, with multiple reconfigurations of non-  
334 planar kerf structures suspended from the ceiling of the space. Furthermore, we examined multiple  
335 non-planar reconfigurable structures by varying the occupant positions. It is demonstrated that the  
336 reconfiguring kerf structures influence RT60 such that the configuration with multiple area

337 divisions has a better acoustic response, especially at 500 Hz and 1000 Hz if echo reduction is  
338 desired in space, and the acoustic response remains consistent regardless of the occupant positions.  
339 Overall, the desired acoustic response can be achieved by varying kerf cut densities and  
340 reconfiguring the kerf structures. The next step will be to explore the association between kerf  
341 structure dynamics reconfigurations and their acoustic response. Another future work will be to  
342 examine the acoustic response of these kerf structures when they are placed in multiple locations  
343 in a space with increased volume.

344

### 345 **Data Availability Statements**

346 Some or all data, models, or codes that support the findings of this study are available from the  
347 corresponding author upon reasonable request.

348

### 349 **Acknowledgments**

350 This material is based upon work supported by the National Science Foundation under CMMI  
351 1912823 and CMMI 1913688. Part of this study was supported by Innovation X Project, at Texas  
352 A&M University. Any opinions, findings, conclusions, or recommendations expressed in this  
353 material are those of the author(s) and do not necessarily reflect the views of the National Science  
354 Foundation.

355

### 356 **References**

357 Anna, G. n.d. "Recommended reverberation times for 7 key spaces." Accessed January 19, 2023.  
358 <https://blog.siniat.com.au/recommended-reverberation-times-for-7-key-space>.  
359 Belanger, Z. M. 2018. "Slumped Glass: Auxetics and Acoustics." *ACADIA // 2018: Recalibration. On imprecision and infidelity. [Proceedings of the 38th Annual Conference of the Association for Computer Aided Design in Architecture (ACADIA) ISBN 978-0-692-17729-7] Mexico City, Mexico 18-20 October, 2018, pp. 244-249*. CUMINCAD.

363 Beranek, L. 2006. "Analysis of Sabine and Eyring equations and their application to concert hall  
364 audience and chair absorption." *The Journal of the Acoustical Society of America*, 120:  
365 1399–1410. <https://doi.org/10.1121/1.2221392>.

366 Capone, M., and E. Lanzara. 2018. *Kerf bending: ruled double curved surfaces manufacturing*.  
367 124.

368 Chen, R., C. Turman, M. Jiang, N. Kalantar, M. Moreno, and A. Muliana. 2020. "Mechanics of  
369 kerf patterns for creating freeform structures." *Acta Mech*, 231 (9): 3499–3524.  
370 <https://doi.org/10.1007/s00707-020-02713-8>.

371 Harten, A. van der. 2013. "Pachyderm Acoustical Simulation: Towards Open-Source Sound  
372 Analysis." *Architectural Design*, 83 (2): 138–139. <https://doi.org/10.1002/ad.1570>.

373 Holterman, A. 2018. "Pattern Kerfing for Responsive Wooden Surfaces: A formal approach to  
374 produce flexible panels with acoustic performance." Master Thesis. Delft University of  
375 Technology.

376 Hung, M. 2017. "Leading the IoT: Gartner Insights on How to Lead in a Connected World."  
377 *online*. [https://www.gartner.com/imagesrv/books/iot/iotEbook\\_digital.pdf](https://www.gartner.com/imagesrv/books/iot/iotEbook_digital.pdf).

378 Ivanovic-Sekularac, J., N. Šekularac, and J. C. Tovarovic. 2012. "Wood as element of façade  
379 cladding in modern architecture." *Technics Technologies Education Management*, 7:  
380 1304–1310.

381 Jakimovska Popovska, V., B. Iliev, and I. Spiroski. 2016. "Characteristics of Medium Density  
382 Fiberboards for Furniture Production and Interior Application." *South East European  
383 Journal of Architecture and Design*, 2016: 1–5.  
384 <https://doi.org/10.3889/seejad.2016.10013>.

385 Jaramillo, A. M., and C. Steel. 2015. *Architectural acoustics*. PocketArchitecture : technical  
386 design series. London ; New York: Routledge.

387 Kalantar, N., and A. Borhani. 2018. "Informing Deformable Formworks - Parameterizing  
388 Deformation Behavior of a Non-Stretchable Membrane via Kerfing." *Learning, Adapting  
389 and Prototyping - Proceedings of the 23rd CAADRIA Conference*, CAADRIA, 339–348.  
390 Tsinghua University, Beijing, China.

391 Olivieri, O., J. Bolton, and T. Yoo. 2006. "Measurement of transmission loss of materials using a  
392 standing wave tube." *INTER-NOISE 2006. The 35th International Congress and  
393 Exposition on Noise Control Engineering*, INTER-NOISE 2006. Honolulu, Hawaii, USA.

394 Peters, B. T. 2011. "Responsive Acoustic Surfaces: Computing Sonic Effects." *RESPECTING  
395 FRAGILE PLACES [29th eCAADe Conference Proceedings / ISBN 978-9-4912070-1-3],  
396 University of Ljubljana, Faculty of Architecture (Slovenia) 21-24 September 2011,  
397 pp.819-828*. CUMINCAD.

398 Quam, R., I. Martínez, C. Lorenzo, B. A, M. Rosa-Zurera, J. P, and A. JL. 2012. "Studying  
399 audition in fossil hominins: A new approach to the evolution of language?" *Psychology  
400 of Language*, 1–37.

401 "Reverberation time | WELL Standard." n.d. Accessed January 29, 2023.  
402 <https://standard.wellcertified.com/comfort/reverberation-time>.

403 SEA. n.d. "HUMAN VOICE FREQUENCY RANGE." <https://seaindia.in/>. Accessed January  
404 19, 2023. <https://seaindia.in/blogs/human-voice-frequency-range/>.

405 Shahid, Z., C. G. Bond, M. S. Johnson, J. E. Hubbard Jr., N. Kalantar, and A. Muliana. 2022a.  
406 "Dynamic Response of Flexible Viscoelastic Kerf Structures of Freeform Shapes."  
407 *International Journal of Solids and Structures*, 111895.  
408 <https://doi.org/10.1016/j.ijsolstr.2022.111895>.

409 Shahid, Z., J. E. Hubbard, N. Kalantar, and A. Muliana. 2022b. "An investigation of the dynamic  
410 response of architectural kerf structures." *Acta Mech*, 233 (1): 157–181.  
411 <https://doi.org/10.1007/s00707-021-03108-z>.

412 Shahid, Z., M. Johnson, C. Bond, J. Hubbard, N. Kalantar, and A. Muliana. 2021. "Dynamic  
413 Responses of Architectural Kerf Structures." *American Society of Composites 36th  
414 Technical Conference*.

415 Varjo, J., V. Hongisto, A. Haapakangas, H. Maula, H. Koskela, and J. Hyönä. 2015.  
416 "Simultaneous effects of irrelevant speech, temperature and ventilation rate on  
417 performance and satisfaction in open-plan offices." *Journal of Environmental  
418 Psychology*, 44: 16–33. <https://doi.org/10.1016/j.jenvp.2015.08.001>.

419 Vercammen, M. L. 2013. "Sound concentration caused by curved surfaces." *Proceedings of  
420 Meetings on Acoustics - The 21st International Congress on Acoustics*, ICA. Montreal,  
421 Canada: Acoustical Society of America.

422 Wulfrank, T., Y. Jurkiewicz, and E. Kahle. 2014. "Design-Focused Acoustic Analysis of Curved  
423 Geometries Using a Differential Raytracing Technique." *Building Acoustics*, 21 (1): 87–  
424 95. SAGE Publications Ltd STM. <https://doi.org/10.1260/1351-010X.21.1.87>.

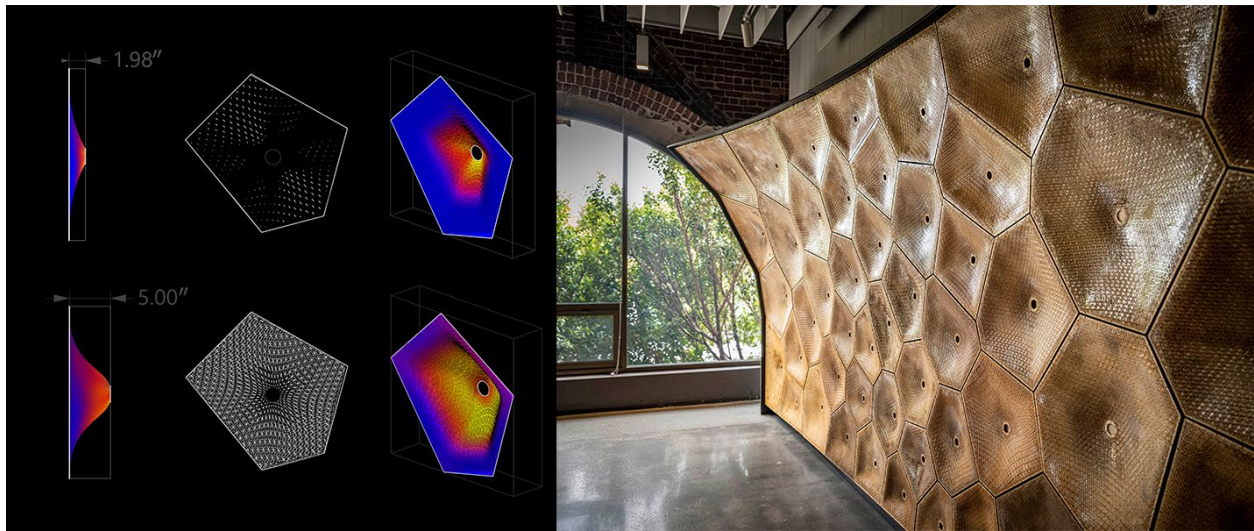
425 Zarrinmehr, S., E. Akleman, M. Ettehad, N. Kalantar, and A. Borhani. 2017a. "Kerfing with  
426 Generalized 2D Meander-Patterns: Conversion of Planar Rigid Panels into Locally-  
427 Flexible Panels with Stiffness Control." *Future Trajectories of Computation in Design  
428 /17th International Conference, CAAD Futures 2017, Proceedings*, CAAD Futures, 276–  
429 293. Istanbul, Turkey.

430 Zarrinmehr, S., E. Akleman, M. Ettehad, N. Kalantar, A. B. Haghghi, and S. Sueda. 2017b. "An  
431 Algorithmic Approach to Obtain Generalized 2D Meander-Patterns." *Bridges 2017  
432 Conference Proceedings. The 20th Annual Bridges Conference*, BRIDGES, 87–94.  
433 Waterloo, Ontario, Canada.

434 Zarrinmehr, S., M. Ettehad, N. Kalantar, A. Borhani, S. Sueda, and E. Akleman. 2017c.  
435 "Interlocked archimedean spirals for conversion of planar rigid panels into locally  
436 flexible panels with stiffness control." *Computers & Graphics*, 66: 93–102.  
437 <https://doi.org/10.1016/j.cag.2017.05.010>.

438

439

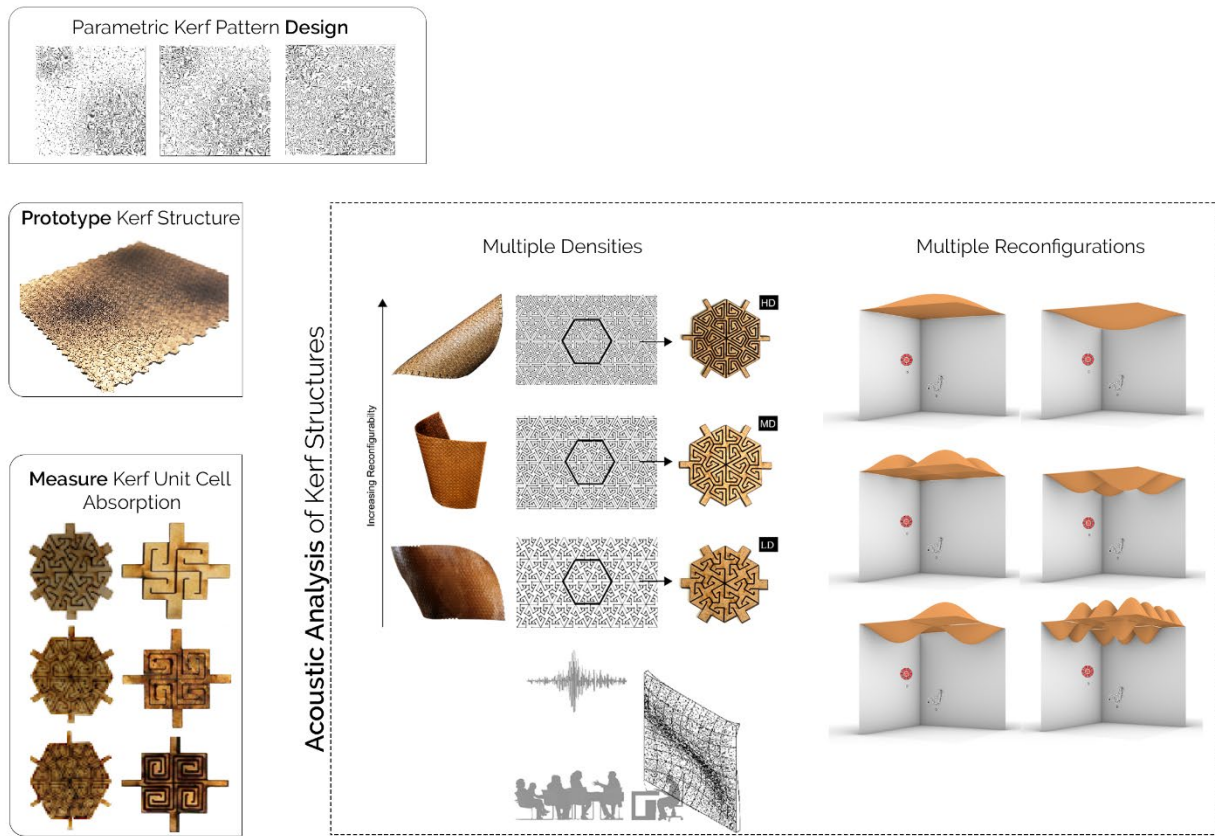


440

441

**Fig. 1.** Creating reconfigurable surfaces from kerf structures

442



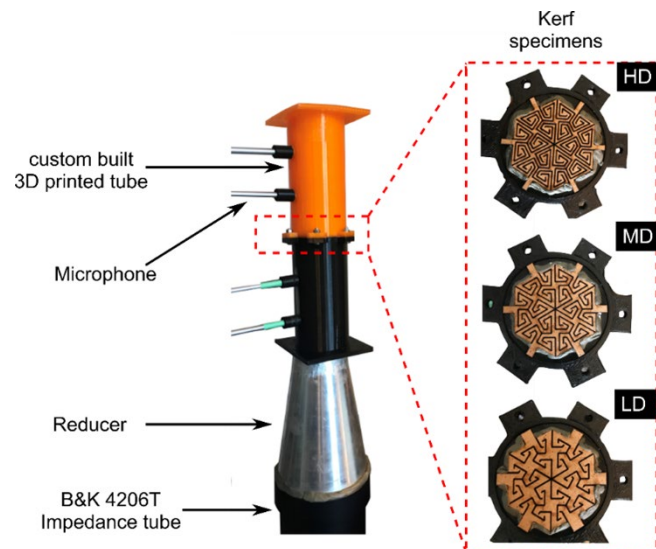
443

444

**Fig. 2.** Design and Assessment of Reconfigurable Kerf Structure

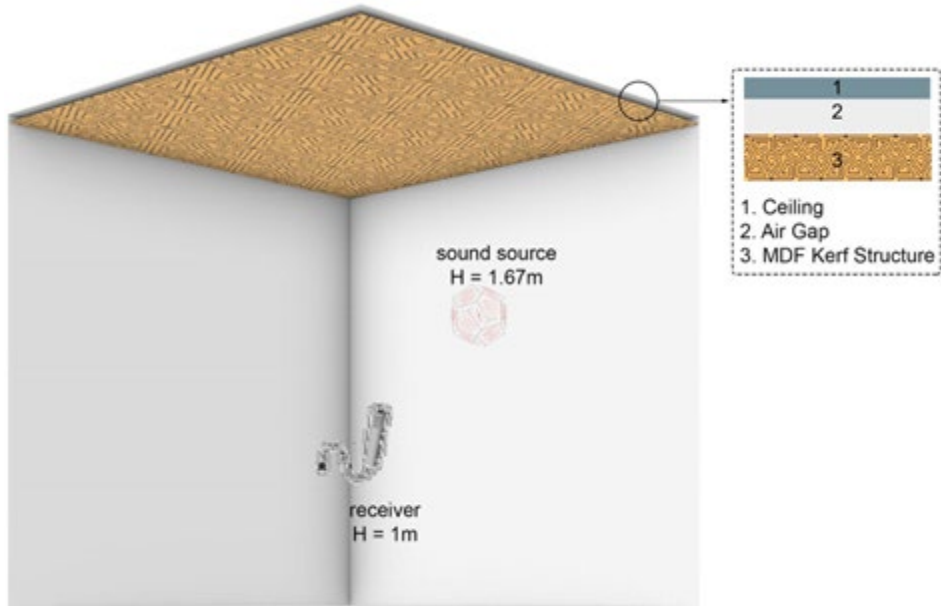
445

446



447 **Fig. 3.** Experimental test setup for measuring the absorption of kerf unit-cells using two-load  
448 method

449



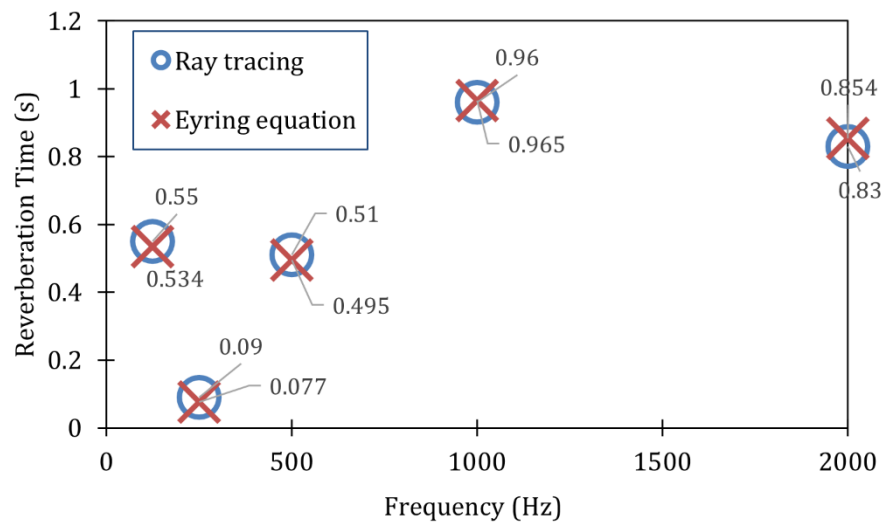
450

451

**Fig. 4.** Model set up for raytracing simulations

452

453

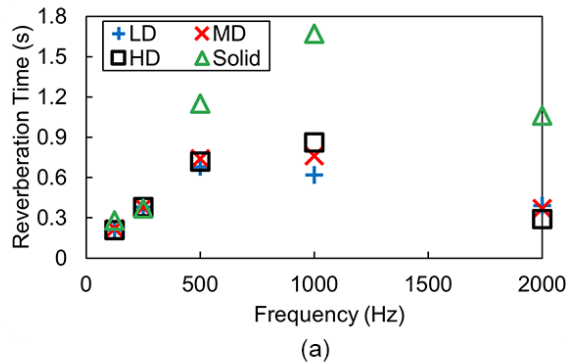


454

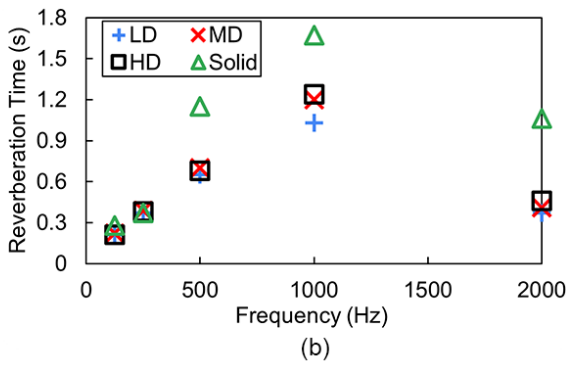
455 **Fig. 5.** Comparison of reverberation times from Ray-tracing simulation and Eyring equation

456 method in a room with solid MDF panels suspended at 24 mm from the ceiling

457



(a)



(b)

458

459 **Fig. 6.** Reverberation times from ray-tracing simulations for different densities of kerf panels  
 460 suspended at: (a) 24 mm, (b) 12 mm

461

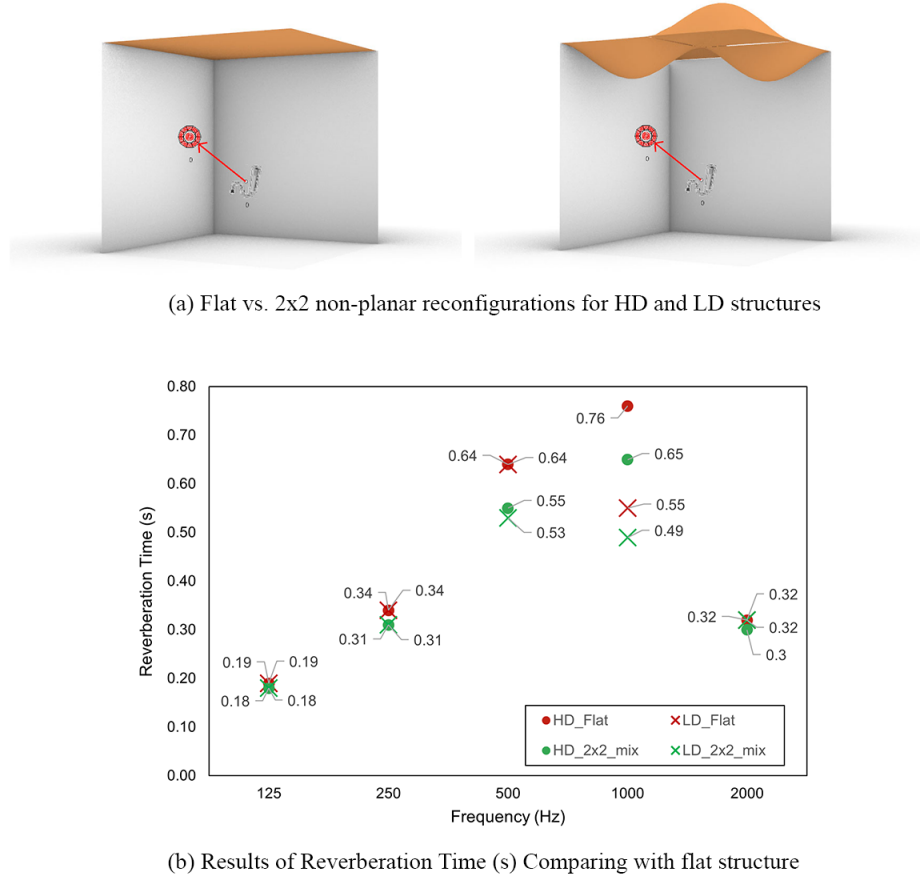
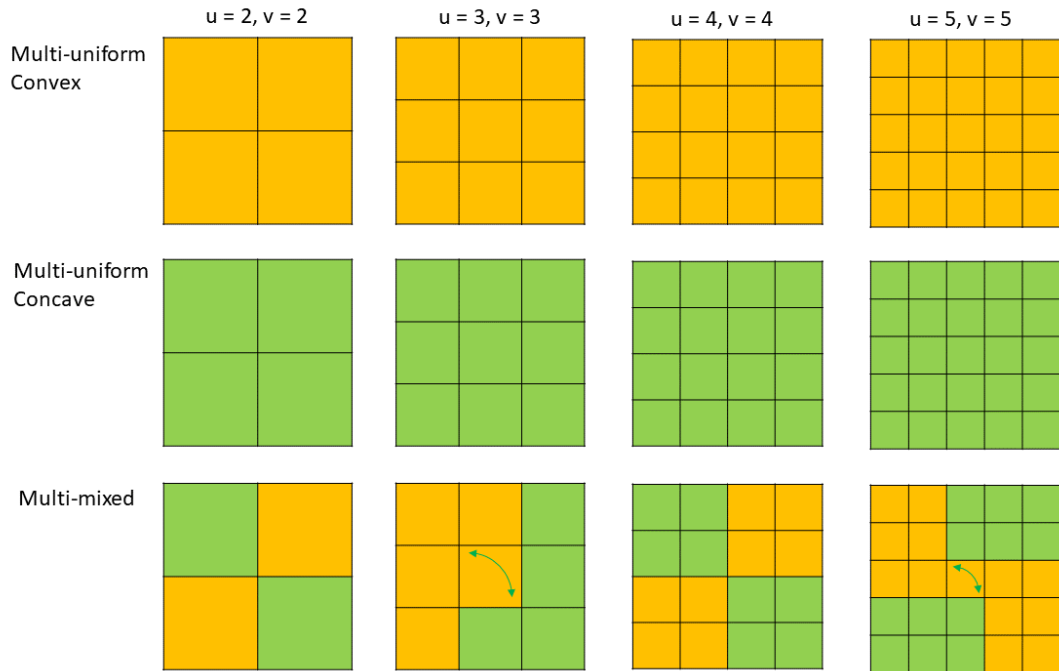


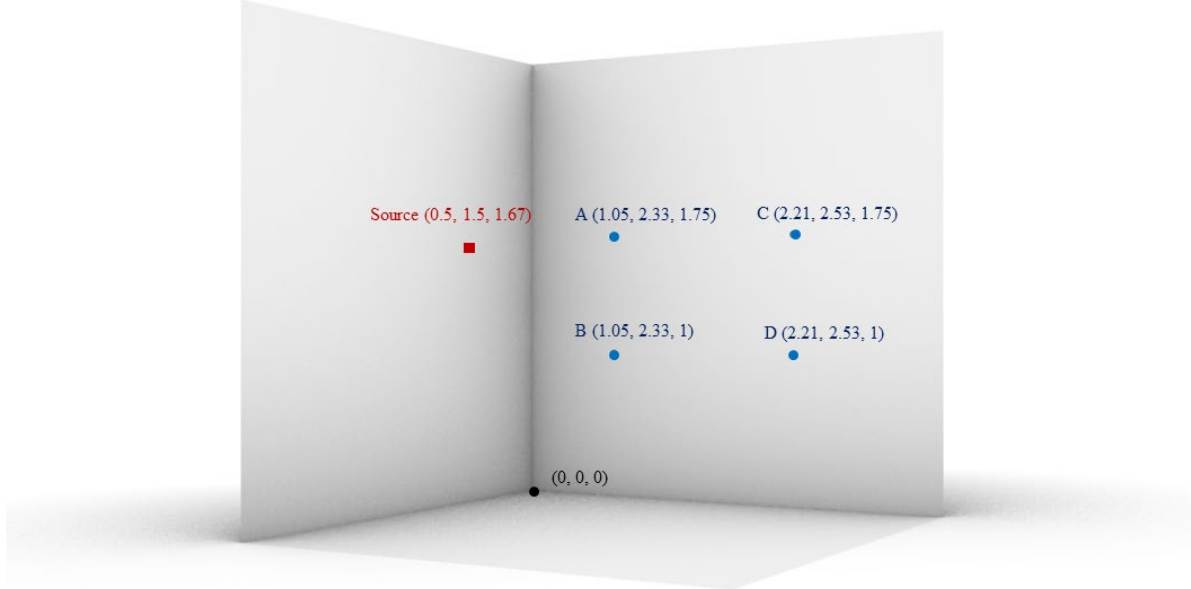
**Fig. 7. Reverberation time of LD and HD reconfigurable kerf structure**



463

464 **Fig. 8.** Three types of non-planar reconfiguration of HD kerf structures suspended 24mm from a  
 465 ceiling in a small office space: (1) Multi-uniform convex: 2x2, 3x3, 4x4, 5x5 (2) Multi-uniform  
 466 concave: 2x2, 3x3, 4x4, 5x5 (3) Multi-mixed: 2x2, 3x3, 4x4, 5x5

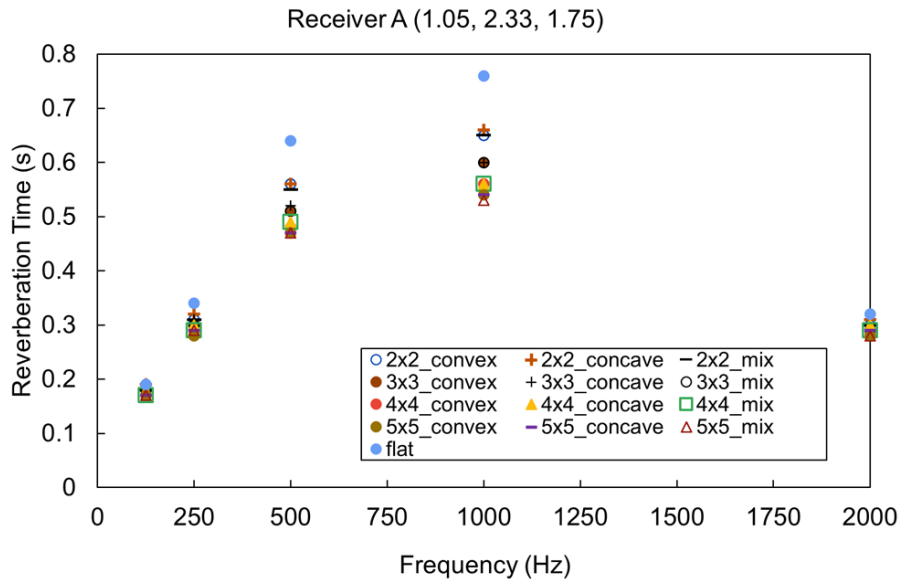
467



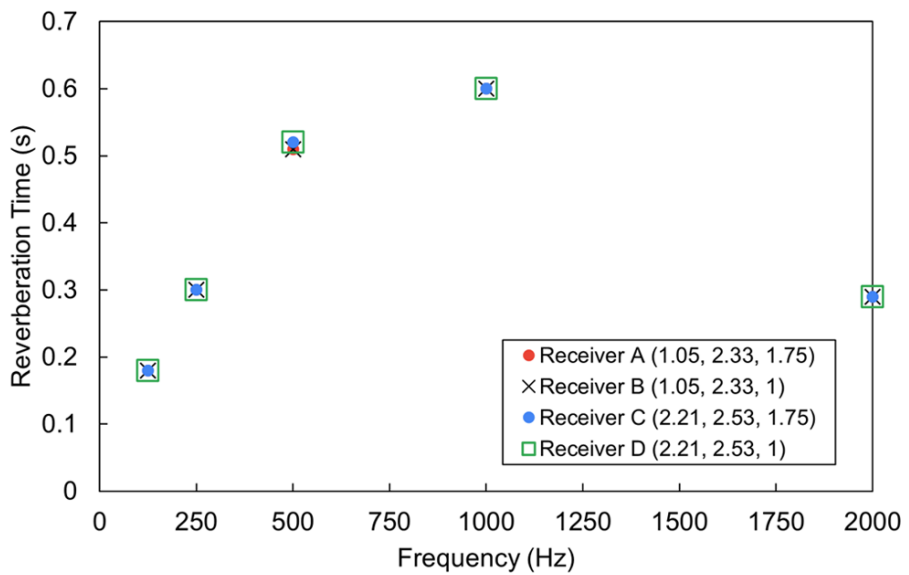
468

469 **Fig. 9.** Perspective View of Spatial Positions of Sound Source and Four Receivers (A, B, C, D)

470



(a) Reverberation Time of all Non-Planar Reconfigurations and Flat surface at Receiver A



(b) Reverberation Time of 3x3 multi-mix reconfiguration at Receiver A, B, C, D

471

472 **Fig. 10.** Comparison of Reverberation times for different types of kerf structure reconfigurations  
 473 for four receiver positions

474

475 **Table 1.** Geometrical properties of hexagonal domain with triangular pattern unit cell (HD, MD,  
476 and LD)

Unit cell	Total surface area ( $\times 10^{-3}m^2$ )	Solid surface area ( $\times 10^{-3}m^2$ )	Air gap area ( $\times 10^{-3}m^2$ )	Ratio of Air gap Total surface area
HD	1.65	1.33	0.32	0.20
MD	1.65	1.45	0.20	0.12
LD	1.65	1.51	0.14	0.08

477

478

479

480

**Table 2.** Absorption coefficients from experiments

Material	Frequency (Hz)					NRC
	125	250	500	1000	2000	
HD MDF	0.54	0.63	0.37	0.32	0.83	0.55
MD MDF	0.51	0.62	0.35	0.38	0.82	0.55
LD MDF	0.57	0.65	0.40	0.51	0.76	0.60

481

482

**Table 3.** Receiver Spatial Locations.

<b>Receiver #</b>	<b>Distance to front wall and one side wall (m)</b>	<b>Height (m) (<math>H_R</math>)</b>	<b>Distance to sound source (m) (<math>D_{SR}</math>)</b>
A	1.05, 2.33	1.75	1
B	1.05, 2.33	1	1
C	2.21, 2.53	1.75	2
D	2.21, 2.53	1.	2

484 Note: see also **Fig. 10.**